Decentralized Control of Distributed Actuation in a Segmented Soft Robot Arm

Azadeh Doroudchi, Sachin Shivakumar, Rebecca E. Fisher, Hamid Marvi,
Daniel Aukes, Ximin He, Spring Berman, and Matthew M. Peet

***Abstract*— Continuum robot manipulators present challenges for controller design due to the complexity of their infinite-dimensional dynamics. This paper develops a practical dynamics-based approach to synthesizing state feedback controllers for a soft continuum robot arm composed of segments with local sensing, actuation, and control capabilities. Each segment communicates its states to its two adjacent neighboring segments, requiring a tridiagonal feedback matrix for decentralized controller implementation. A semi-discrete numerical approximation of the Euler-Bernoulli beam equation is used to represent the robot arm dynamics. Formulated in state space representation, this numerical approximation is used to define an H_∞ optimal control problem in terms of a Bilinear Matrix Inequality. We develop three iterative algorithms that solve this problem by computing the tridiagonal feedback matrix which minimizes the H_∞ norm of the map from disturbances to regulated outputs. We confirm through simulations that all three controllers successfully dampen the free vibrations of a cantilever beam that are induced by an initial sinusoidal displacement, and we compare the controllers' performance.**

I. INTRODUCTION

Continuum robots [32], [33] have high-dimensional configuration spaces, which can be leveraged to achieve versatile functionality over a wide variety of configurations. The implementation of *decentralized control architectures* [2], [26] in continuum robots would enable scalability of the robot design, minimize expensive communication and power overhead, and increased robustness to partial failure. Furthermore, continuum robots composed of *soft materials* would exhibit high structural compliance in response to environmental inputs that can enhance the robot's functionality. Soft continuum robots with decentralized controllers can be used in manufacturing, surgery, and other applications requiring flexible manipulators that can operate safely in close proximity to humans. They can also be used to perform unstructured manipulation and locomotion tasks in uncertain, dynamic environments. Furthermore, novel soft materials such as smart hydrogels [12], which can dramatically change volume and other properties in response to stimuli such as temperature, pH, and chemicals, present the possibility of constructing soft continuum robots with on-demand dynamic control of local properties through continuous sensing and actuation that is distributed throughout the robot. Such robots could offer new capabilities through self-regulated adaptive reconfiguration.

Challenges remain in the design of decentralized controllers for soft continuum robots. While there are many scalable and compliant soft robot designs, these designs are typically model-independent or use simplified models which do not accurately reflect either the nonlinear dynamics of highly deformable robots or the practical issues of sensor and actuator design and placement [16], [18], [24]. In addition, most soft robot designs still require complex sensing, control, and actuation to achieve even low-dimensional configuration spaces. Dynamic models of continuum robots would facilitate a variety of control techniques. However, many of the control-oriented models developed for these types of robots have thus far been governed by kinematic equations describing rigid links [9], [22], [34], and hence are not useful for designing feedback controllers when both the forces produced by the actuators and the motion of the robot are distributed throughout the structure. While dynamic models have been formulated, e.g. a Partial Differential Equation (PDE) model of bending in a hyper-redundant continuum robotic arm [14], their complexity often prevents their practical implementation in controller design and motion planning [32], [33].

Work on the control of vibrations in beams [7], [8] is closely related to the decentralized control strategies that we design in this paper. The optimal sensor/actuator placement problem has been well-studied in vibration control; see, e.g. [6], [17]. In addition, there has been significant research on the question of how to construct stabilizing decentralized feedback laws for a given network and, furthermore, whether there are necessary and sufficient conditions for the existence of such local feedback laws. The largest class of systems for which we know the answer to this question are those systems which are *quadratically invariant* [19], [23]. While testing quadratic invariance is known to be NP-hard, in practice, testing quadratic invariance under sparsity constraints for reasonably-sized systems is not difficult and furthermore, certain well-studied sparsity patterns are known

This work was supported by Office of Naval Research (ONR) Award N00014-17-1-2117.

Azadeh Doroudchi is with the School of Electrical, Computer and Energy Engineering, Arizona State University, Tempe, AZ 85287, USA {adoroudc@asu.edu}. Sachin Shivakumar, Hamid Marvi, Spring Berman, and Matthew M. Peet are with the School for Engineering of Matter, Transport and Energy, Arizona State University, Tempe, AZ 85287, USA {sshivak8, hmarvi, spring.berman, mpeet}@asu.edu. Rebecca E. Fisher is with the Department of Basic Medical Sciences, University of Arizona College of Medicine-Phoenix, Phoenix, AZ 85004, USA and the School of Life Sciences, Arizona State University, Tempe, AZ 85287, USA {rfisher@email.arizona.edu}. Daniel Aukes is with the Polytechnic School, Arizona State University, Mesa, AZ 85212, USA {daukes@asu.edu}. Ximin He is with the Department of Materials Science and Engineering, University of California, Los Angeles, CA 90095, USA {ximinhe@ucla.edu}.

to be quadratically invariant, with the most well-known case being when the controller is diagonal or both the controller and plant are upper- or lower-tridiagonal. Unfortunately, however, the tridiagonal sparsity constraint generated by discretization of beam-type equations (with zeros everywhere except the diagonal and first off-diagonal elements) is not quadratically invariant. Because the decentralized control problem with tridiagonal structure is difficult, the literature on vibration control of beams focuses on the case of diagonal decentralization, in which neighboring controllers do not communicate with each other.

We are interested in designing decentralized controllers with tridiagonal structure for soft robot arms. Since the tridiagonal structure is not quadratically invariant, we instead consider the non-convex Bilinear Matrix Inequality (BMI) formulation of the problem and design algorithms to solve this BMI directly using iteration and gradient descent.

Many algorithms have been developed for finding local solutions to BMI problems, several focusing on Branch and Bound [10], [28], [29], [30], [31]. However, many such global optimization algorithms have high computational complexity, making them impractical for the large state spaces induced by spatial discretization of a PDE [20]. For high dimensional problems, Yamada et al. suggest a modified triangle-covering based algorithm which reduces the computational cost [35]. Unfortunately, however, this approach is restricted to a class of Bilinear Matrix Inequalities (BMIs) that does not include the decentralized controller synthesis problem. The method proposed in [15] and the rank minimization approach in [13] will both typically converge to a local optimum given an initial feasible controller. Other approaches involve linearization of the BMI [11]. However many of these methods, as shown in [25], can fail to converge to even locally optimal solutions.

In this work, we develop a novel practical approach to designing decentralized state feedback controllers for soft continuum robot arms composed of segments with local sensing, actuation, and control capabilities. The control objective is to regulate the robot arm's displacement in the presence of disturbance inputs; i.e., to dampen its disturbance-induced vibrations. Our approach does not require the use of a complex nonlinear model that describes the infinite-dimensional dynamics of the robot. Instead, we represent the robot arm's spatiotemporal dynamics using a semi-discrete numerical approximation of the Euler-Bernoulli beam PDE (Section II). This numerical approximation is formulated as an ordinary differential equation (ODE) state space model for implementation in linear matrix inequality (LMI) methods. The state space model is used to define an H_∞ optimal control problem in terms of a BMI (Section III). We present three algorithms of increasing stability and performance that solve this problem by computing the tridiagonal feedback matrix which minimizes the H_∞ norm of the map from disturbances to regulated outputs (Section IV). Finally, we simulate the controllers computed by each algorithm for the case of a cantilever beam composed of hydrogel material and compare their performance (Section V). We conclude with a discussion of the simulation results and directions for future work (Section VI).

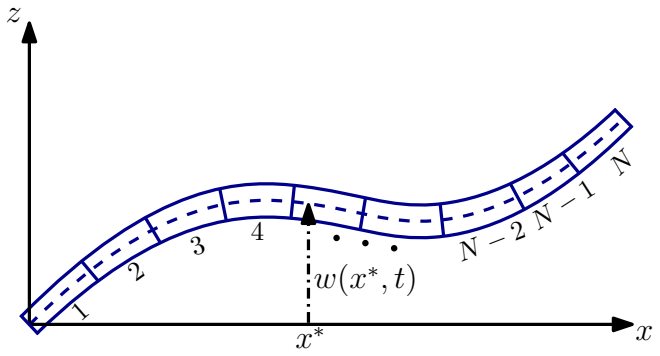

Fig. 1: Semi-discrete beam model with N segments.

II. DYNAMIC MODEL

The robot arm is constructed from N identical cylindrical segments that are arranged in a series configuration, as illustrated in Fig. 1. We assume that each segment is equipped with sensing, actuation, control, and communication elements. We also assume that each segment can apply local torques and can measure local deformations. For example, when a segment is composed of force-sensitive conductive hydrogel [12], local deformations can be sensed from a resulting change in resistivity across the segment, and this change in resistivity provides an electrical signal which can be used as an output to a local feedback controller. The local controller can then induce a current, which causes local temperature changes in the segment that produce prescribed deformations and resulting torques.

In this decentralized sensing and actuation model of a soft robot arm, we likewise impose a decentralized communication architecture with a similar chain topology, meaning that each segment can exchange state measurements only with adjacent segments.

A. Model definition

To model the segmented robot arm, we will use a discretized version of the cantilever beam, wherein the beam is composed of material that is elastic, homogeneous, and isotropic. The beam is composed of material with Young's modulus E and density ρ. The beam has length L and a uniform cross-section of area A_c, and area moment of inertia I about the neutral axis.

Let $w(x,t)$ be the transverse displacement (see Fig. 1) of point $x \in [0, L]$ on the beam at time $t \in [0, T]$, where T is a specified final time. The PDE describing a one-dimensional unforced Euler-Bernoulli beam is given by

$$b^2 \frac{\partial^4 w}{\partial x^4} + \frac{\partial^2 w}{\partial t^2} = 0, \qquad b^2 = \frac{EI}{\rho A_c}. \tag{1}$$

We define boundary conditions for this model that describe a cantilever beam, in which the deflection and slope of the

fixed end and the bending moment and shear force at the free end are all set to zero:

$$\begin{aligned} w(0,t) &= 0, \qquad \frac{\partial^2 w}{\partial x^2}(L,t) = 0, \\ \frac{\partial w}{\partial x}(0,t) &= 0, \quad \frac{\partial^3 w}{\partial x^3}(L,t) = 0, \end{aligned} \tag{2}$$

where $t \in [0, T]$.

We note that the Euler-Bernoulli beam equation is linear, assumes small shear stresses and is only accurate for small deflections. However, it has been shown in [3] that for a uniform circular cross-section with diameter D, when $L \geq 20D$ the Euler-Bernoulli beam model yields a reasonably accurate approximation of the robot arm dynamics when the material properties satisfy certain assumptions. Furthermore, we note that the use of the robust control framework in this paper mitigates the effect of inaccuracy in the model.

B. State space representation

To represent the segmented arm, we construct a discretized approximation of the continuum PDE beam model (1), (2), which results in a set of linear ODEs. As in [5], we apply the central finite difference method with second-order accuracy to obtain a semi-discrete space approximation of model (1), (2) (discrete in the spatial coordinate x and continuous in time t). We define $h = L/N$ as the length of each segment and x_j as the x position of the right boundary of segment $j \in \{1, ..., N\}$. Then we have that $x_j = jh$ for each segment j, and we define $x_0 = 0$. For the boundary conditions, we also introduce two external points $x_{-1} = -h$ and $x_{N+1} = L + h$. The semi-discretization version of model (1) is then given by the following system of N linear equations, each describing the dynamics of the transverse displacement of point x_j on the beam at time $t \in [0, T]$:

$$\begin{aligned} \ddot{w}(x_j,t) = &-\frac{b^2}{h^4}[w(x_{j+2},t) - 4w(x_{j+1},t) + 6w(x_j,t) \\ &- 4w(x_{j-1},t) + w(x_{j-2},t)], \quad j = 1, ..., N. \end{aligned} \tag{3}$$

Note that the dynamics of each segment's displacement is approximated as a function of its own displacement and that of the two closest segments on either side. The boundary conditions (2) are expressed as

$$\begin{aligned} &w(x_0,t) = 0, \quad w(x_{-1},t) = -w(x_1,t), \\ &w(x_{N+1},t) = w(x_N,t), \quad w(x_{N+2},t) = w(x_{N-1},t). \end{aligned} \tag{4}$$

We define the system state variables as $w(x_j, t)$, $\dot{w}(x_j, t)$, $j = 1, ..., N$ and arrange them in the vectors $w = [w(x_1,t)\ w(x_2,t)\ ...\ w(x_N,t)]^T$, $\dot{w} = [\dot{w}(x_1,t)\ \dot{w}(x_2,t)\ ...\ \dot{w}(x_N,t)]^T$. The system of equations (3) and the boundary conditions (4) can then be represented in state space form as follows:

$$\begin{bmatrix} \dot{w} \\ \ddot{w} \end{bmatrix} = \begin{bmatrix} A_{11} & A_{12} \\ A_{21} & A_{22} \end{bmatrix} \begin{bmatrix} w \\ \dot{w} \end{bmatrix} \tag{5}$$

where

$$\begin{aligned} A_{11} &= [0]_{N\times N}, \qquad A_{12} = I_{N\times N}, \\ A_{21} &= \frac{-b^2}{h^4} A_h, \quad A_{22} = [0]_{N\times N}, \end{aligned}$$

and the matrix $A_h \in \mathbb{R}^{N\times N}$ is defined as

$$A_h = \begin{bmatrix} 5 & -4 & 1 & 0 & 0 & 0 & 0 & 0 & \cdots & 0 \\ -4 & 6 & -4 & 1 & 0 & 0 & 0 & 0 & \cdots & 0 \\ 1 & -4 & 6 & -4 & 1 & 0 & 0 & 0 & \cdots & 0 \\ 0 & 1 & -4 & 6 & -4 & 1 & 0 & 0 & \cdots & 0 \\ 0 & 0 & 1 & -4 & 6 & -4 & 1 & 0 & \cdots & 0 \\ \vdots & \ddots & \ddots & \ddots & \ddots & \ddots & \ddots & \ddots & \ddots & \vdots \\ 0 & \cdots & 0 & 0 & 1 & -4 & 6 & -4 & 1 & 0 \\ 0 & \cdots & 0 & 0 & 0 & 1 & -4 & 6 & -4 & 1 \\ 0 & \cdots & 0 & 0 & 0 & 0 & 1 & -4 & 6 & -3 \\ 0 & \cdots & 0 & 0 & 0 & 0 & 0 & 1 & -3 & 2 \end{bmatrix}.$$

Including inputs and outputs, we obtain a state space representation given by

$$\begin{bmatrix} \dot{w} \\ \ddot{w} \end{bmatrix} = A \begin{bmatrix} w \\ \dot{w} \end{bmatrix} + Bu, \qquad y = C \begin{bmatrix} w \\ \dot{w} \end{bmatrix} + Du, \tag{6}$$

in which the system control input is denoted by $u \in \mathbb{R}^N$ and the output by $y \in \mathbb{R}^{2N}$. The A, B, C, and D matrices are defined as

$$\begin{aligned} A &= \begin{bmatrix} A_{11} & A_{12} \\ A_{21} & A_{22} \end{bmatrix}_{2N\times 2N}, \quad B = \begin{bmatrix} [0]_{N\times N} \\ I_{N\times N} \end{bmatrix}_{2N\times N}, \\ C &= I_{2N\times 2N}, \qquad D = \begin{bmatrix} [0]_{N\times N} \\ I_{N\times N} \end{bmatrix}_{2N\times N}. \end{aligned} \tag{7}$$

In Section III, we discuss how the decentralized communication constraint leads to structural constraints on the gain from input to output.

III. CONTROLLER SYNTHESIS

In this section, we use the linear ODE model developed in Section II-B to define a decentralized control problem assuming local full-state feedback. We first impose the mild assumption that the uncontrolled system is neutrally stable and controllable. To define the H_∞-optimal control problem, we use the standard regulator framework, yielding the 2-input, 2-output system representation $R \in \mathbb{R}^{7N\times 7N}$ as:

$$R = \left[\begin{array}{c|cc} A & B_1 & B_2 \\ \hline C_1 & D_{11} & D_{12} \\ C_2 & D_{21} & D_{22} \end{array}\right], \tag{8}$$

where

$$\begin{aligned} B_1 &= \begin{bmatrix} B & 0 \end{bmatrix}_{2N\times 4N}, \quad B_2 = B, \\ C_1 &= \begin{bmatrix} C \\ 0 \end{bmatrix}_{3N\times 2N}, \qquad C_2 = C, \\ D_{11} &= \begin{bmatrix} D & 0 \\ 0 & 0 \end{bmatrix}_{3N\times 4N}, \ D_{12} = \begin{bmatrix} D \\ I \end{bmatrix}_{3N\times N}, \\ D_{21} &= \begin{bmatrix} D & I \end{bmatrix}_{2N\times 4N}, \ D_{22} = D. \end{aligned}$$

Because $C_2 = I$, the control problem is one of full-state feedback. The control problem, then, is to find the feedback controller $u = Ky$, $K \in \mathbb{R}^{N\times 2N}$, that minimizes the H_∞ norm of the map from disturbing inputs u to regulated outputs y. However, we now add a communication constraint in which we specify the structure of K to be tridiagonal (NOT block-diagonal). This structure implies that

the moment generated by each segment is based only on measurements of its own state and the states of its two neighboring segments. Define the set of tridiagonal matrices as

$$T := \{K \in \mathbb{R}^{n\times n} \; : \; K = \begin{bmatrix} k_{1,1} & k_{1,2} & 0 & \cdots & 0 & 0 & 0 \\ k_{2,1} & k_{2,2} & k_{2,3} & \cdots & 0 & 0 & 0 \\ 0 & k_{3,2} & k_{3,3} & \cdots & 0 & 0 & 0 \\ \vdots & \vdots & \vdots & \ddots & \vdots & \vdots & \vdots \\ 0 & 0 & 0 & \cdots & k_{n-2,n-2} & k_{n-2,n-1} & 0 \\ 0 & 0 & 0 & \cdots & k_{n-1,n-2} & k_{n-1,n-1} & k_{n-1,n} \\ 0 & 0 & 0 & \cdots & 0 & k_{n,n-1} & k_{n,n} \end{bmatrix}, \; k_{i,j} \in \mathbb{R}\} \tag{9}$$

We now denote the set of admissible controller gains by S, where

$$S := \{\, [K_1 \; K_2] \;\mid\; K_1, K_2 \in T \,\}.$$

This allows us to represent the controller information constraint as $K \in S$.

We may now formulate the H_∞ optimal control problem as a Bilinear Matrix Inequality (BMI). By using the bounded-real lemma, it can be shown that γ is an H_∞ norm bound of the transfer function from input to output if there exists a positive definite matrix P and controller K which satisfy the BMI constraint (10) [4]. Consequently, we can formulate the optimization problem (10) below, whose solution is the H_∞-optimal decentralized controller $K^* \in S$.

minimize $\gamma > 0$ such that

$$\begin{bmatrix} (A+B_2K)^TP + P(A+B_2K) & *^T & *^T \\ B_1^TP & -\gamma I & *^T \\ (C_1+D_{12}K) & D_{11} & -\gamma I \end{bmatrix} < 0 \tag{10}$$

for some $K \in S$ and $P > 0$.

In the matrix inequality, " $*$ " is used to represent symmetric elements of the matrix.

IV. Proposed Algorithms for Solving the BMI

The optimization problem (10) is a BMI in the matrix variables K and P. Solving BMIs is known to be an NP-hard problem [27]. In this section, we evaluate three possible algorithms for obtaining locally optimal solutions to this BMI, two based on iteration and one based on gradient descent.

A. Initialization

In all three algorithms, we require an initial feasible solution to the BMI. Furthermore, the selection of initial values can significantly influence convergence to an optimal solution. Unfortunately, however, there are no canonical rules for finding an initial feasible solution.

In our algorithm, we address this problem as follows. Under the assumption that the nominal system is controllable, the following LMI has solution $P > 0$:

$$\text{controllability:} \quad A^TP + PA - BB^T < 0 \tag{11}$$

We use this solution as an estimate of the initial value of P (P_0). Using this P_0 to find the initial value of K (K_0) is problematic, however, because of the additional constraint $K \in S$. To resolve this, we initialize K without the sparsity constraint and solve the resulting LMI version of (10) for P, and then use this as our new estimate of P_0. Given this new value of P_0, we solve the resulting LMI version of (10) for K with the relaxed constraint that only the last row of K is required to have the sparsity structure $K \in S$ of the tridiagonal matrix (9). Using this K, we solve the LMI version of (10) for P. This procedure is repeated by progressively constraining more rows of K to have the structure of the corresponding row of matrix (9) until the entire matrix K has the desired tridiagonal structure.

We have developed the following three algorithms to obtain an H_∞ optimal solution for K. The algorithms all use the initialization procedure described above.

B. Iterative optimization algorithm

Algorithm 1 is a standard iteration-based method used to solve a bilinear system of equations. It is similar to our initialization procedure for the variables P and K. Initializing a value for P (P_0) yields the LMI from (10), which is solved by optimizing over K. Afterward, we fix K in (10) and optimize over P. These steps are repeated until the values of K and P converge to optimal values, at which point the change in γ is minimal.

This algorithm has two drawbacks: it does not converge for certain initial values of P (P_0), especially if the A matrix is numerically ill-conditioned, and the solution for K could have a large magnitude that makes the feedback controller physically impractical to implement. However, imposing additional constraints on the magnitude of K could potentially cause the H_∞ norm to diverge. We next propose two modified versions of this algorithm that address these problems.

C. Modified iterative optimization algorithm

Algorithm 1, depending on the choice of P_0, can end up oscillating between suboptimal solutions for K. This was observed to happen for poor choices of P_0. To reduce these oscillations, we define P and K at each iteration as weighted averages of their current values and their optimized values, obtained by solving the optimization problem (10) during the current iteration. The weight factor α is chosen to be a value between 0 and 1. The α value can be selected to produce small changes in the solution between iterations, thus preventing the solution from making large jumps in the non-convex subspace. An α close to 0 would result in very small changes in P and K over successive iterations.

Algorithm 1 Standard iterative algorithm

Choose a small $\epsilon > 0$. Initialize P to P_0.
while $|\gamma_k - \gamma_{k-1}| > \epsilon$ **do**
  Use the last known value for P.
  Solve for K in problem (10), minimizing γ.
  Use the solution for K in the next step.
  Solve for P in problem (10), minimizing γ.
  γ_k is the minimized value of γ in step 6.
  $k = k + 1$
end while

D. Gradient descent algorithm

Although both Algorithms 1 and 2 are quick to converge, they do not converge at all when the matrices A and B are numerically ill-conditioned. In addition, the solution for K computed by these procedures often has a magnitude that is too large for implementation in practice. We address this problem in Algorithm 3 by splitting optimization problem (10) into two optimization problems with LMI constraints, shown below. The difference here is that we can directly restrict changes in the solution over successive iterations and also limit the values taken by the variables. We redefine the optimization variables as $\Delta K \in \mathbb{R}^{N\times 2N}$ and $\Delta P \in \mathbb{R}^{2N\times 2N}$, whose L_∞-norms are constrained to be small in order to prevent large changes in K and P between iterations.

minimize $\gamma_a > 0$ such that $\|\Delta K\| < \epsilon_1$ and

$$\begin{bmatrix} (A+B_2K_a)^TP + P(A+B_2K_a) & *^T & *^T \\ B_1^TP & -\gamma_a I & *^T \\ (C_1+D_{12}K_a) & D_{11} & -\gamma_a I \end{bmatrix} < 0 \tag{12}$$

for some $K_a \in S$, where $K_a \equiv K + \Delta K$.

minimize $\gamma_b > 0$ such that $\|\Delta P\| < \epsilon_2$ and

$$\begin{bmatrix} (A+B_2K)^TP_a + P_a(A+B_2K) & *^T & *^T \\ B_1^TP_a & -\gamma_b I & *^T \\ (C_1+D_{12}K) & D_{11} & -\gamma_b I \end{bmatrix} < 0 \tag{13}$$

for some $P_a > 0$, where $P_a \equiv P + \Delta P$.

In these two problems, ϵ_1 and ϵ_2 are small positive numbers.

The optimization procedure is performed alternately over ΔK and ΔP as follows such that γ converges to a local minimum. At the beginning of each iteration, problem (12) is solved for ΔK using the current values of K and P, and then K is increased by ΔK. Next, problem (13) is solved for ΔP, and P is increased by ΔP.

V. SIMULATION RESULTS

We validated our numerical approximation of the beam model and investigated the performance of our decentralized state feedback controllers in simulation. *YALMIP* [21], an optimization toolbox for MATLAB with the *MOSEK* solver [1], was used to solve the optimization problems in Algorithms 1, 2, and 3. The beam model was simulated using the MATLAB *lsim* command with $N = 40$ segments and the parameters listed in Table I, where E and ρ are defined for hydrogel material[1].

Algorithm 2 Modified iterative algorithm

Choose a small $\epsilon > 0$ and $\alpha \in (0, 1)$. Initialize P to P_0.
while $|\gamma_k - \gamma_{k-1}| > \epsilon$ **do**
  Use the last known value for P.
  Solve for K in problem (10), minimizing γ.
  $K_{k+1} = K_k + \alpha(K - K_k)$
  Use K_{k+1} as the current value of K.
  Solve for P in problem (10), minimizing γ.
  $P_{k+1} = P_k + \alpha(P - P_k)$
  γ_k is the optimal value of γ in step 7.
  $k = k + 1$
end while

Algorithm 3 Gradient descent algorithm

Choose a small $\epsilon > 0$. Initialize K to K_0 and P to P_0.
while $|\gamma_k - \gamma_{k-1}| > \epsilon$ **do**
  Solve problem (12), minimizing γ_a.
  $K = K + \Delta K$
  Solve problem (13), minimizing γ_b.
  $P = P + \Delta P$
  γ_k is the optimal value of γ_b.
  $k = k + 1$
end while

A. Validation of semi-discrete approximation of beam model

In order to evaluate the accuracy of the numerical approximation (3), (4), we compare it to the analytical solution of the cantilever Euler-Bernoulli beam model (1), (2). The initial conditions of the beam model were set to

$$w(x,0) = \sin\left(\frac{3\pi}{2L}x\right), \quad \frac{\partial w}{\partial t}(x,0) = 0, \quad x \in [0, L]. \tag{14}$$

For these initial conditions, the solution to the beam model (1), (2) can be obtained using the separation of variables method:

$$w(x,t) = \sin\left(\frac{3\pi}{2L}x\right)\cos\left(\frac{9\pi^2 b}{4L^2}t\right), \ t \in [0, T], \ x \in [0, L]. \tag{15}$$

[1]N-isopropylacrylamide, variously abbreviated PNIPA, PNIPAAm, NIPA, PNIPAA or PNIPAm

TABLE I: Beam material and geometric properties

Parameter	Definition	Value	Units
E	Young's modulus at $25°C$	5.0	kPa
ρ	Mass density	1.1	g/cm^3
D	Diameter	5.0	cm
L	Length	1.0	m
A_c	Cross-section area	19.6	cm^2
I	Area moment of inertia	30.7	cm^4

This solution describes the first mode shape of the beam. In the simulations, we set $T = 20$.

Figures 2(a),(b) plot the vibrations of the beam over time from the analytical solution (15) and the numerical approximation, respectively. Figure 2(c) plots the error between the analytical solution and the numerical approximation. Although this error grows over time due to numerical approximation error propagation, it remains relatively small (the magnitude does not exceed 0.08 m within the first 5 s) compared to the maximum amplitude of the beam vibrations within the first few seconds of the simulation, when the controllers effectively damp the vibrations (see next section). Thus, the numerical approximation is sufficiently accurate for use in our optimization methods to synthesize the controllers. Note that a relatively coarse spatial discretization ($N = 40$ segments) was used for the numerical approximation; a closer match to the analytical solution could be achieved with a finer discretization.

B. Comparison of optimal decentralized controllers for damping beam vibrations

Decentralized state feedback controllers were synthesized with Algorithms 1, 2, and 3, and the beam dynamics were simulated for each controller using the numerical approximation (6). All the variables were initialized using the procedure described in Section IV-A.

Figures 3a, 4a, and 5a plot the evolution of the closed-loop H_∞ norm bound, γ, over the execution of each algorithm when the optimization is performed alternately over the variables K and P during each iteration. Figures 3b, 4b, and 5b display the resulting closed-loop beam response for each controller given the initial condition (14). These figures show that all controllers successfully dampen the beam vibrations that are induced by the initial beam displacement within the first 5 seconds. From the convergence rates of the plots in Fig. 3a, 4a, and 5a, it is evident that Algorithm 1 is the least computationally intensive procedure, followed by Algorithm 2 and then by Algorithm 3. This is because K is least constrained in Algorithm 1, which therefore permits large changes in K between iterations and hence has the fastest convergence, followed by the other two algorithms. Algorithm 2 shows superior performance to Algorithm 1, in that it converged to a controller with a smaller H_∞ norm bound ($\gamma = 1.05$, versus $\gamma = 1.42$ for Algorithm 1) at the expense of a slight increase in computational demands. Algorithm 3 converged to the highest H_∞ norm bound ($\gamma = 2.31$) of the three methods since the controller gain values were subject to additional constraints. However, the controller computed by this algorithm would be the most feasible one to implement in practice, since the constraints limit the magnitudes of the controller gains.

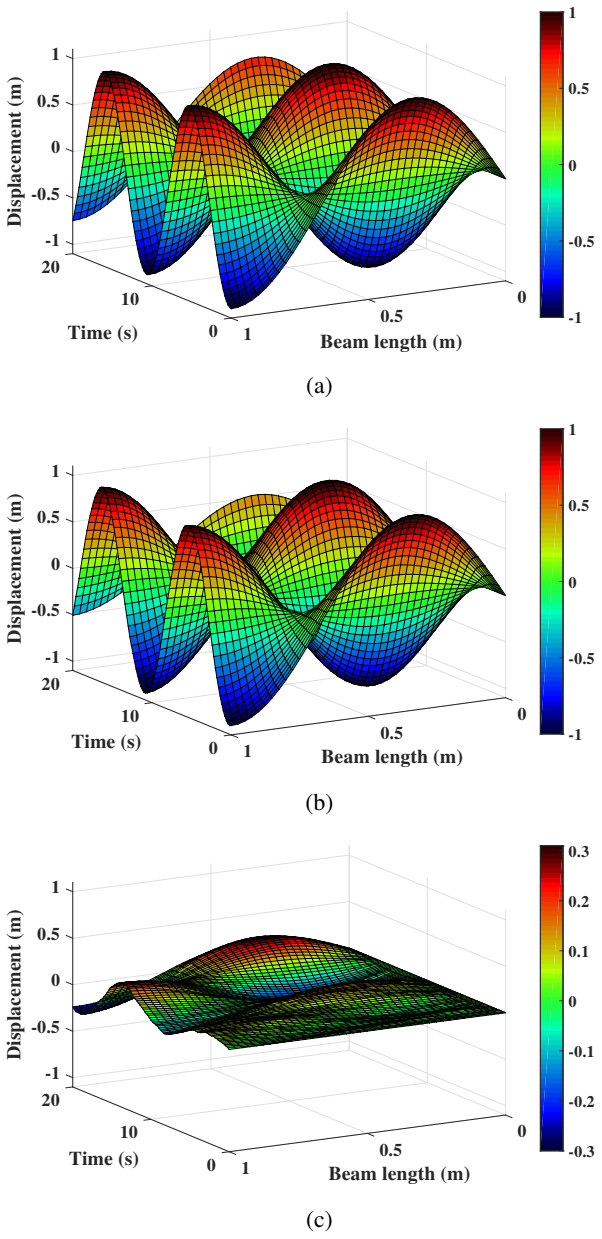

Fig. 2: Euler-Bernoulli cantilever beam free vibrations from (a) the analytical solution (15) and (b) the numerical approximation (3), (4); (c) error between the analytical solution and numerical approximation.

VI. CONCLUSIONS

In this paper, we developed three algorithms for synthesizing a decentralized controller for the discretized Euler-Bernoulli beam model by solving an H_∞ optimal control problem. We found that when the system matrix is numerically ill-conditioned, which is a common property of discretized beam models, convergence of the H_∞ norm is not always guaranteed. In addition, we found that iterative approaches are in general sensitive to the initial selections of P and K. The modifications proposed in the algorithms solved these problems of convergence and sensitivity for the discretized beam model. The iterative and modified iterative methods quickly reach a converged H_∞ norm value, but they do not guarantee convergence for different selections of initial P and K. The gradient descent approach, while

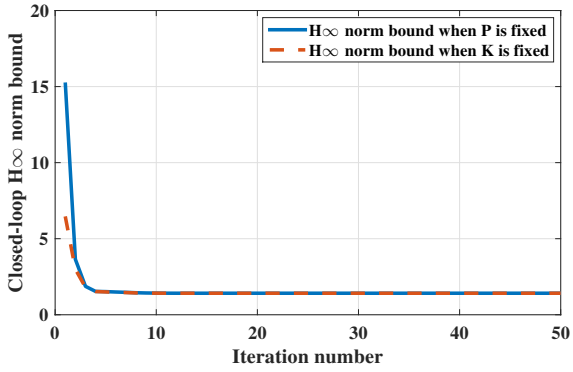

(a)

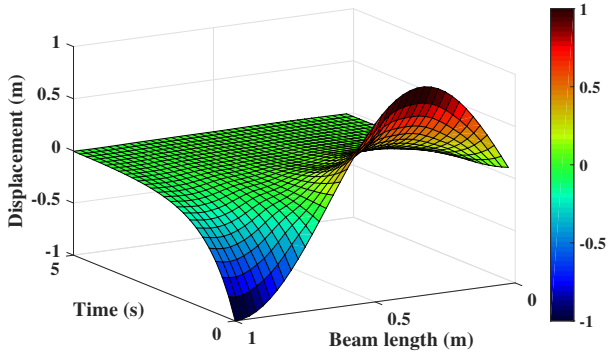

(b)

Fig. 3: (a) H_∞ norm bound converging in the two alternating steps of Algorithm 1. (b) Closed-loop response of the simulated beam with initial conditions (14) and the controller from Algorithm 1.

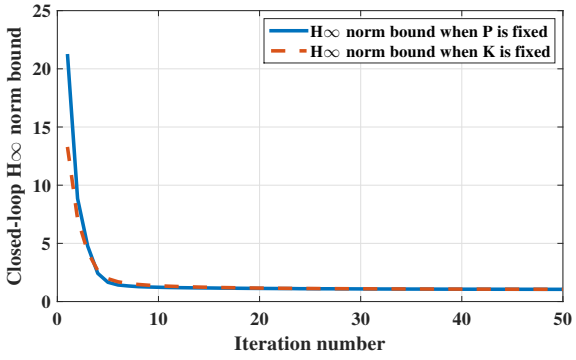

(a)

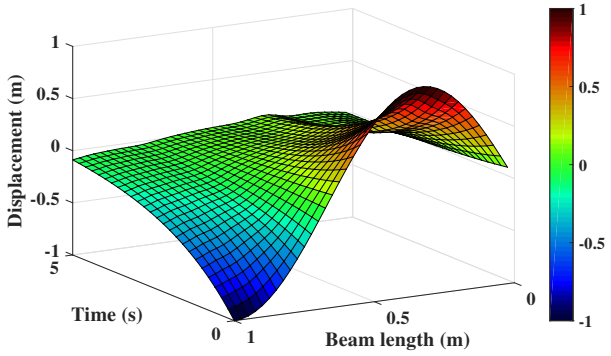

(b)

Fig. 4: (a) H_∞ norm bound converging in the two alternating steps of Algorithm 2. (b) Closed-loop response of the simulated beam with initial conditions (14) and the controller from Algorithm 2.

slightly slower at reaching a converged H_∞ norm value, is less sensitive to different choices of initial P and K. It provides a bounded solution for the controller gains, which is often a necessity in physical systems.

In future work, we plan to develop decentralized controllers for beam models that more accurately describe the dynamics of a soft continuum robot arm composed of hydrogel. We will design these controllers to produce diverse types of arm motions and deformations that are useful for manipulation and locomotion tasks.

VII. ACKNOWLEDGMENTS

The authors gratefully acknowledge Prof. Marc Mignolet for helpful discussions on structural dynamics of beam models and Roozbeh Khodambashi for information about hydrogel functional properties.

REFERENCES

[1] MOSEK ApS. *The MOSEK optimization toolbox for MATLAB manual. Version 8.1.*, 2017.

[2] Lubomir Bakule. Decentralized control: An overview. *Annual Reviews in Control*, 32(1):87–98, 2008.

[3] Eduardo Bayo. Timoshenko versus Bernoulli beam theories for the control of flexible robots. In *Proceedings of IASTED International Symposium on Applied Control and Identification*, pages 178–182, 1986.

[4] Stephen Boyd, Laurent El Ghaoui, Eric Feron, and Venkataramanan Balakrishnan. *Linear matrix inequalities in system and control theory*, volume 15. SIAM, 1994.

[5] Ioan Bugariu, Sorin Micu, and Ionel Rovenţa. Approximation of the controls for the beam equation with vanishing viscosity. *Mathematics of Computation*, 85(301):2259–2303, 2016.

[6] Neda Darivandi, Kirsten Morris, and Amir Khajepour. An algorithm for LQ optimal actuator location. *Smart Materials and Structures*, 22(3):035001, 2013.

[7] Jeffrey J. Dosch, Daniel J. Inman, and Ephrahim Garcia. A self-sensing piezoelectric actuator for collocated control. *Journal of Intelligent Material Systems and Structures*, 3(1):166–185, 1992.

[8] Wouter P. Engels, Oliver N. Baumann, Stephen J. Elliott, and R. Fraanje. Centralized and decentralized control of structural vibration and sound radiation. *The Journal of the Acoustical Society of America*, 119(3):1487–1495, 2006.

[9] Isuru S. Godage, Gustavo A. Medrano-Cerda, David T. Branson, Emanuele Guglielmino, and Darwin G. Caldwell. Modal kinematics for multisection continuum arms. *Bioinspiration & Biomimetics*, 10(3):035002, 2015.

[10] Keat-Choon Goh, Michael G. Safonov, and George P. Papavassilopoulos. A global optimization approach for the BMI problem. In *Proceedings of the 33rd Conference on Decision and Control (CDC)*, volume 3, pages 2009–2014. IEEE, 1994.

[11] Arash Hassibi, Jonathan How, and Stephen Boyd. A path-following method for solving BMI problems in control. In *Proceedings of the American Control Conference (ACC)*, volume 2, pages 1385–1389. IEEE, 1999.

[12] Ximin He, Michael Aizenberg, Olga Kuksenok, Lauren D. Zarzar, Ankita Shastri, Anna C. Balazs, and Joanna Aizenberg. Synthetic homeostatic materials with chemo-mechano-chemical self-regulation. *Nature*, 487(7406):214, 2012.

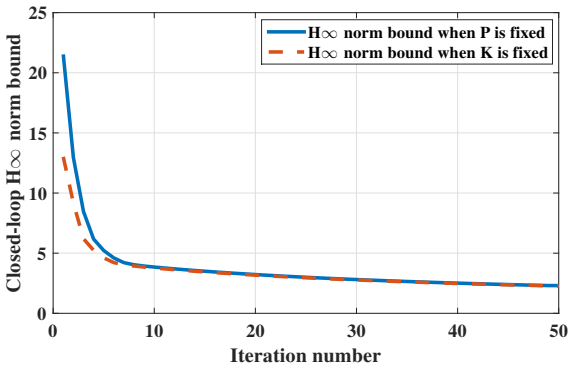

(a)

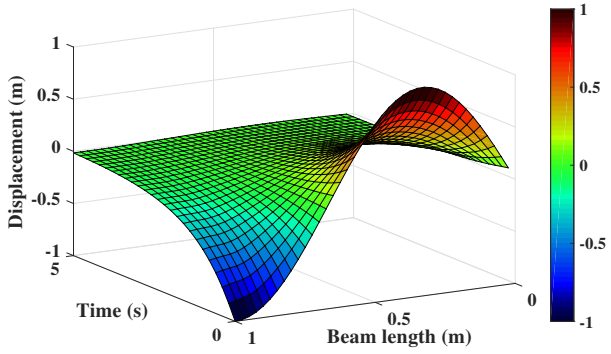

(b)

Fig. 5: (a) H_∞ norm bound converging in the two alternating steps of Algorithm 3. (b) Closed-loop response of the simulated beam with initial conditions (14) and the controller from Algorithm 3.

[13] Soichi Ibaraki and Masayoshi Tomizuka. Rank minimization approach for solving BMI problems with random search. In *Proceedings of the American Control Conference (ACC)*, volume 3, pages 1870–1875. IEEE, 2001.

[14] Mircea Ivanescu, Nirvana Popescu, and Decebal Popescu. The shape control of tentacle arms. *Robotica*, 33(3):684–703, 2015.

[15] Stoyan Kanev, Carsten Scherer, Michel Verhaegen, and Bart De Schutter. Robust output-feedback controller design via local BMI optimization. *Automatica*, 40(7):1115–1127, 2004.

[16] Sangbae Kim, Cecilia Laschi, and Barry Trimmer. Soft robotics: a bioinspired evolution in robotics. *Trends in Biotechnology*, 31(5):287–294, 2013.

[17] K. Ramesh Kumar and S. Narayanan. The optimal location of piezoelectric actuators and sensors for vibration control of plates. *Smart Materials and Structures*, 16(6):2680, 2007.

[18] Cecilia Laschi and Matteo Cianchetti. Soft robotics: new perspectives for robot bodyware and control. *Frontiers in Bioengineering and Biotechnology*, 2:3, 2014.

[19] Laurent Lessard and Sanjay Lall. Quadratic invariance is necessary and sufficient for convexity. In *Proceedings of the American Control Conference (ACC)*, pages 5360–5362. IEEE, 2011.

[20] Shih-Mim Liu and George P. Papavassilopoulos. Numerical experience with parallel algorithms for solving the BMI problem. *IFAC Proceedings Volumes*, 29(1):1827–1832, 1996.

[21] Johan Lofberg. YALMIP: a toolbox for modeling and optimization in MATLAB. In *Proceedings of International Symposium on Computer Aided Control Systems Design*, pages 284–289. IEEE, 2004.

[22] Fumitoshi Matsuno and Kentaro Suenaga. Control of redundant 3D snake robot based on kinematic model. In *Proceedings of International Conference on Robotics and Automation (ICRA)*, volume 2, pages 2061–2066. IEEE, 2003.

[23] Michael Rotkowitz, Randy Cogill, and Sanjay Lall. Convexity of optimal control over networks with delays and arbitrary topology. *International Journal of Systems, Control and Communications*, 2(1-3):30–54, 2010.

[24] Daniela Rus and Michael T. Tolley. Design, fabrication and control of soft robots. *Nature*, 521(7553):467, 2015.

[25] Michael G. Safonov, Keat-Choon Goh, and J. H. Ly. Control system synthesis via bilinear matrix inequalities. In *Proceedings of the American Control Conference (ACC)*, volume 1, pages 45–49. IEEE, 1994.

[26] Dragoslav D. Siljak. *Decentralized control of complex systems*. Courier Corporation, 2011.

[27] Onur Toker and Hitay Ozbay. On the NP-hardness of solving bilinear matrix inequalities and simultaneous stabilization with static output feedback. In *Proceedings of the American Control Conference (ACC)*, volume 4, pages 2525–2526. IEEE, 1995.

[28] Hoang Duong Tuan, Pierre Apkarian, and Y. Nakashima. A new Lagrangian dual global optimization algorithm for solving bilinear matrix inequalities. *International Journal of Robust and Nonlinear Control*, 10(7):561–578, 2000.

[29] Jeremy G. VanAntwerp and Richard D. Braatz. A tutorial on linear and bilinear matrix inequalities. *Journal of Process Control*, 10(4):363–385, 2000.

[30] Jeremy G. VanAntwerp, Richard D. Braatz, and Nikolaos V. Sahinidis. Globally optimal robust control for systems with time-varying nonlinear perturbations. *Computers & Chemical Engineering*, 21:S125–S130, 1997.

[31] Jeremy G. VanAntwerp, Richard D. Braatz, and Nikolaos V. Sahinidis. Globally optimal robust process control. *Journal of Process Control*, 9(5):375–383, 1999.

[32] Ian D. Walker. Continuous backbone "continuum" robot manipulators. *ISRN Robotics*, 2013. volume 2013.

[33] Ian D. Walker, Howie Choset, and Gregory S. Chirikjian. Snake-like and continuum robots. In *Springer Handbook of Robotics*, pages 481–498. Springer, 2016.

[34] Robert J. Webster III and Bryan A. Jones. Design and kinematic modeling of constant curvature continuum robots: A review. *The International Journal of Robotics Research*, 29(13):1661–1683, 2010.

[35] Yuji Yamada and Shinji Hara. Global optimization for H_∞ control with constant diagonal scaling. *IEEE Transactions on Automatic Control*, 43(2):191–203, 1998.